






Titin-truncating mutations associated with dilated cardiomyopathy alter length-dependent activation and its modulation via phosphorylation

Petr G. Vikhorev ^{1*}, Natalia N. Vikhoreva², WaiChun Yeung¹, Amy Li³, Sean Lal⁴, Cristobal G. dos Remedios ⁵, Cheavar A. Blair⁶, Maya Guglin⁶, Kenneth S. Campbell ⁶, Magdi H. Yacoub¹, Pieter de Tombe ^{1,2,7}, and Steven B. Marston ¹

¹National Heart and Lung Institute, Imperial College London, Du Cane Road, London W12 0NN, UK; ²Heart Science Centre, Magdi Yacoub Institute, Harefield Hospital, London UB9 6JH, UK; ³Department of Pharmacy and Biomedical Sciences, La Trobe University, Bendigo, VIC 3550, Australia; ⁴School of Medical Sciences, Faculty of Medicine and Health, University of Sydney, NSW 2006, Australia; ⁵Division of Molecular Cardiology and Biophysics, Victor Chang Cardiac Research Institute, Darlinghurst, NSW 2010, Australia; ⁶Division of Cardiovascular Medicine, Department of Physiology, University of Kentucky, Lexington, KY, USA; and ⁷Department of Physiology and Biophysics, University of Illinois at Chicago, Chicago, IL, USA

Received 8 November 2019; editorial decision 13 October 2020; accepted 20 October 2020; online publish-ahead-of-print 2 November 2020

Time for primary review: 24 days

Aims

Dilated cardiomyopathy (DCM) is associated with mutations in many genes encoding sarcomere proteins. Truncating mutations in the titin gene *TTN* are the most frequent. Proteomic and functional characterizations are required to elucidate the origin of the disease and the pathogenic mechanisms of *TTN*-truncating variants.

Methods and results

We isolated myofibrils from DCM hearts carrying truncating *TTN* mutations and measured the Ca^{2+} sensitivity of force and its length dependence. Simultaneous measurement of force and adenosine triphosphate (ATP) consumption in skinned cardiomyocytes was also performed. Phosphorylation levels of troponin I (TnI) and myosin binding protein-C (MyBP-C) were manipulated using protein kinase A and λ phosphatase. mRNA sequencing was employed to overview gene expression profiles. We found that Ca^{2+} sensitivity of myofibrils carrying *TTN* mutations was significantly higher than in myofibrils from donor hearts. The length dependence of the Ca^{2+} sensitivity was absent in DCM myofibrils with *TTN*-truncating variants. No significant difference was found in the expression level of *TTN* mRNA between the DCM and donor groups. *TTN* exon usage and splicing were also similar. However, we identified down-regulation of genes encoding Z-disk proteins, while the atrial-specific regulatory myosin light chain gene, *MYL7*, was up-regulated in DCM patients with *TTN*-truncating variants.

Conclusion

Titin-truncating mutations lead to decreased length-dependent activation and increased elasticity of myofibrils. Phosphorylation levels of TnI and MyBP-C seen in the left ventricles are essential for the length-dependent changes in Ca^{2+} sensitivity in healthy donors, but they are reduced in DCM patients with *TTN*-truncating variants. A decrease in expression of Z-disk proteins may explain the observed decrease in myofibril passive stiffness and length-dependent activation.

* Corresponding author. Tel: +44 (0)20 7594 2736; E-mail: p.vikhorev@imperial.ac.uk

© The Author(s) 2020. Published by Oxford University Press on behalf of the European Society of Cardiology.

This is an Open Access article distributed under the terms of the Creative Commons Attribution License (<http://creativecommons.org/licenses/by/4.0/>), which permits unrestricted reuse, distribution, and reproduction in any medium, provided the original work is properly cited.

Table 1 Patient characteristics

Heart sample	ID	Gene	Mutation	Sex	Age (years)	Diagnosis and clinical notes
DCM						
D12	4.047	MYOM1	E247K	F	63	Familial DCM, LVEF 20%, NYHA IV, LVEDD 87 mm, LVESD 78 mm, ventricular tachycardia, dual pacemakers. No acute myocardial infarction or ischaemic heart disease, areas of full thickness fibrosis, normal coronary arteries. Severe left ventricular dilation. No diabetes.
D16	7.036			M	56	Idiopathic DCM, LVEF 5–20%. LVEDD 78 mm, LVESD 58 mm, FS 15–20%, CO 3.2 L/min, CI 1.7. Implantable cardioverter-defibrillator, ischaemic heart disease, viral, severe global dilatation. No diabetes.
DCM TTNtv						
D6	4.100	TTN	p.(R24390Tfs*41)	M	22	Familial DCM, six close relatives also developed DCM, post-viral cardiomyopathy, LVEF 15%, no coronary artery disease. No diabetes.
D7	4.125	TTN	p.(R24390Tfs*41)	M	37	Familial DCM, LVEF 15%, NYHA IV, severe dilation of all four heart chambers, severe systolic impairment of both ventricular chambers. No diabetes.
D9	2.029	TTN	p.(Y19850*)	F	22	Familial DCM, LVEF 13–20%, NYHA III, CO 5.1 L/min, CI 3.2 L/min/m ² , impaired systolic, moderate LV dilation, 3-year history. Ventricular tachycardia, dual-chamber pacemaker, no myocardial infarction. Diabetes status is unknown. No ischaemia present.
D28	3.133	TTN	p.(N23731Kfs*5)	F	60	Familial DCM, LVEF 25%, LVEDD 64 mm, LVESD 54 mm, FS 16%, CO 1.9 L/min, CI 1.1 L/min/m ² , diagnosis 9 years, atrial fibrillation 6 months. Diabetes status is unknown. Possible ischaemia with signs of previous infarcts and occluded epicardial artery.

TTN mutations are numbered according to Refseq NP_001243779.

CI, cardiac index; CO, cardiac output; FS, fractional shortening; LVEDD, left ventricular end-diastolic diameter; LVEF, left ventricular ejection fraction; LVESD, left ventricular end-systolic diameter; NYHA, New York Heart Association.

TTNtv and the total titin expression was unchanged.^{15,24,33} However, cardiovascular stress may play a role in the clinical manifestation of DCM in this group of patients. Experiments with the use of a mouse model with a *TTN* truncation mutation showed that administration of angiotensin II stimulated left ventricular dilatation, systolic dysfunction, and myocardial fibrosis.³³

The Frank–Starling law of the heart states that the force of cardiac contraction increases with diastolic volume and cardiomyocyte length.³⁴ However, neither the proteins involved nor the mechanism of the length-dependent activation is currently well understood.³⁵

Recently, attention has focused on the super-relaxed state of myosin,³⁶ which is characterized by very slow ATPase activity. Myosin light chain kinase, via phosphorylation of the myosin regulatory light chains (MYL2), may regulate the number of myosin heads in the super-relaxed state.^{36,37} It is also possible that the super-relaxed state can be regulated via phosphorylation of MyBP-C.³⁸

The objective of this research was to determine the effects of truncating mutations in the *TTN* gene on the Ca²⁺ sensitivity of force, length-dependent activation, and their modulation by PKA catalysed phosphorylation in myofibril preparations from the hearts of DCM patients (Table 1). We also estimated the kinetic parameters of myofibril contraction. Transcriptomic approach was used to help us understand the molecular mechanisms involved in the disease process. All titin-truncating

mutations included in this study are located in the A-band region of titin.²⁴

2. Methods

2.1 Patient and donor clinical characteristics

Left ventricular tissue was obtained from explanted hearts of patients diagnosed with familial or idiopathic DCM (4.100, 4.125, 2.029, 3.133, 4.047, 7.036, 2.008, 4.121) from the Sydney Heart Bank.³⁹ Donor hearts had no history of cardiac disease and were obtained when no suitable transplant recipient was found (Supplementary material online, Table S1). All samples from heart transplant patients were cryopreserved within minutes of the loss of coronary circulation. Donor heart samples were from the University of Kentucky (24713, CF462, D0F54, D612E, BC90C, 4B3FA) and the Sydney Heart Bank (5.138, 5.089, 5.128, 5.090, 6.008, 4.083, 5.131, 4.104, 5.084, 7.080, 5.003, 5.054, 5.126, 5.048, 5.086). Patients provided written informed consent under ethical approvals obtained by the University of Sydney and the University of Kentucky. The investigation conformed with the principles outlined in the Declaration of Helsinki. Human research ethics approval was obtained from the NHS National Research Ethics Service, South West

London REC3 (10/H0803/147); the Imperial College Healthcare Tissue Bank (HTA license 12275, REC approval 17/WA/0161); the University of Sydney (HREC #2012/2814); and the University of Kentucky, USA (08-03338-F2L). The mutations in the *TTN* gene were discovered earlier by whole-exome sequencing.⁴⁰ Fifty-eight genes implicated in DCM were screened for potentially disease-causing variants, and no other mutations were found in the studied cohort of patients with *TTN*tv,⁴⁰ suggesting that *TTN*tv are the most likely cause of DCM in these patients.

2.2 mRNA sequencing

mRNA extraction, quality control, library preparation, and sequencing (Illumina HiSeq 2x150 bp, to an average depth of approximately 54 million reads per sample) were performed by GENEWIZ (South Plainfield, NJ, USA). Sequencing quality and mapping statistics are summarized in the [Supplementary material online, Table S2](#). DESeq2^{41,42} was used to compare gene expression between the healthy donor ($n = 6$; mean age 33 ± 10 years, 50% male) and patient groups of samples ($n = 4$; mean age was 35 ± 9 years, 50% male). The data were analysed for alternative splicing using DEXSeq.⁴³ RNA-Seq reads were mapped to the human hg38 genome assembly.

2.3 Gel electrophoresis and western blotting

Phos-tag SDS polyacrylamide gel electrophoresis and western blotting were performed using standard methods.^{22,44} The primary antibodies used for western blotting were cardiac anti-TnI mouse monoclonal antibody P4-14G5 (ThermoFisher/Invitrogen, MA1-20119), anti-MyBPC3 mouse monoclonal antibody G-7 (Santa Cruz, sc-137237), and anti-myosin light chain 2 rabbit monoclonal antibody (Abcam, ab183490). The membranes were treated with HRP-linked secondary anti-mouse (GE Healthcare, NA931) or anti-rabbit (Abcam, ab205718) antibodies and visualised using ECL western blotting detection reagent (Amersham) or SuperSignal West Pico PLUS Chemiluminescent Substrate (Thermo Fisher Scientific). Images were recorded with the Syngene G: box gel documentation system and analysed using GeneTools software. Phosphatase inhibitor PhosSTOP (Roche) was added during sample preparation to preserve MYL2 phosphorylation.

2.4 Preparation of single myofibrils

Myofibrils were prepared from frozen left ventricular tissue according to a published procedure.⁴⁵ Myofibrils were stored in rigor solution on ice until use within 2 days.

2.5 Phosphorylation and dephosphorylation of myofibrils in vitro

Myofibrils were phosphorylated with PKA catalytic subunits from bovine heart (Merck, P2645; 500 Units/mL) at 20°C for 20 min in a solution containing (mmol/L): 10 MOPS (pH 7.0), 10 EGTA, 5 DTT, 5 Mg-ATP, and 1 free Mg^{2+} . Protein dephosphorylation was achieved using incubation with λ phosphatase (New England Biolabs, P07503; 1000 U/mL) at 20°C for 40 min in a solution containing (mmol/L): 10 MOPS (pH 7.0), 5 DTT, 3 Mn^{2+} , 0.1 Mg^{2+} , and 20 2,3-butanedione monoxime. Following incubation, myofibrils were pelleted, the supernatant removed, and the myofibril pellet resuspended and stored in rigor solution: 10 Tris (pH 7.1), 132 NaCl, 5 KCl, 1 $MgCl_2$, 5 EGTA, 5 dithiothreitol (DTT), and 10 NaN_3 . All solutions were supplemented with protease inhibitors (μ mol/L): 10 chymostatin, 5 pepstatin, 40 leupeptin, 10 E-64, and 200 PMSF.

2.6 Single myofibril mechanics

The apparatus for the measurement of force and passive stiffness in single myofibrils has been previously described.⁴⁵ A single myofibril or small bundle was suspended horizontally using two specially prepared glass microtools. Contraction and relaxation were initiated by a rapid Ca^{2+} concentration jump achieved by a fast solution switch system. The mechanical force data were fit to the Hill equation: $F = F_0 + F_{max} [Ca^{2+}]^{n_H} / (EC_{50}^{n_H} + [Ca^{2+}]^{n_H})$, where F is steady-state developed force, F_{max} is the maximum saturated value F can attain, EC_{50} is the concentration of Ca^{2+} at which F attains 50% of F_{max} , and n_H is the Hill coefficient. Information on myofibril kinetics is provided in [Supplementary material online, Methods](#). Measurement of passive force was performed as described previously.²⁴ Experiments were performed at 17°C.⁴⁶

Relaxing (0.1 μ mol/L free Ca^{2+}) and activating (0.4–15.8 μ mol/L free Ca^{2+}) solutions contained (in mmol/L): 10 MOPS (pH 7.0), 5 Mg-ATP, 1 free Mg^{2+} , 5 DTT, 10 phosphocreatine, 0.5 mg/mL creatine kinase, 1 unit/mL bacterial purine nucleoside phosphorylase, and 0.5 7-methylguanosine. The Ca-EGTA:EGTA ratio was set to obtain 10 mmol/L total EGTA and the desired free $[Ca^{2+}]$. K-propionate and Na_2SO_4 were added to adjust the ionic strength of the solution to 200 mmol/L. The relaxing solution in the bath chamber (0.01 μ mol/L free Ca^{2+}) was supplemented with (in μ mol/L): 10 chymostatin, 5 pepstatin, 40 leupeptin, 10 E-64, and 200 PMSF.

2.7 Simultaneous measurement of force and myosin ATPase in cardiac strips

The experimental apparatus for simultaneous measurements of force and myosin ATPase in cardiac fine strips have previously been described in detail.⁴⁷ More information is provided in the [Supplementary material online](#).

2.8 Statistical analysis

Statistics analysis and graphs were prepared using Prism 7 (GraphPad Software, San Diego, CA, USA). Data are expressed as means \pm SEMs. One-way ANOVA followed by Fisher's least significant difference multiple comparison test was used for multiple group comparison. The Student's *t*-test was used to compare two groups of normally distributed variables; otherwise, the Mann–Whitney *U*-test was used. The linear mixed model analysis was used to compare patient and donor groups. The model was fit using the restricted maximum likelihood method. Patient and donor samples were entered to the model as random factors. Disease, treatment type, and sarcomere length were considered as fixed factors. The analysis was performed using SPSS Statistics software (IBM, version 26), and estimated means are reported. In this case, data are shown as estimated means \pm SEMs. *P*-values of <0.05 were considered statistically significant. The Wald test was used to generate *P*-values and log2 fold changes in gene expression. Genes with an adjusted *P*-value <0.05 and absolute log2 fold change >1 were called differentially expressed genes.

3. Results

3.1 Gene expression

The four heterozygous *TTN* mutations (samples D6, D7, D9, and D28) result in premature termination of mRNA translation. We performed mRNA sequencing on the samples of left ventricular heart tissue used for the functional measurements to examine gene expression patterns and *TTN* alternative exon usage. A stop codon can lead to non-sense-

mediated decay of the mRNA or production of truncated titin proteins. However, we did not find significant down-regulation of the *TTN* gene in the DCM samples ($n = 4$) with frameshift mutations compared to healthy donor heart samples ($n = 6$; [Supplementary material online, Table S3](#)). Additionally, the samples with *TTN* mutations were very similar to the exon usage of healthy donor hearts ([Supplementary material online, Figure S1 and Table S3](#)). However, differences were observed in the expression of several other genes ([Supplementary material online, Table S4](#)) that might explain the aetiology. We found that the gene *MYL7* that encodes atrial-specific myosin regulatory light chain 2 (MLC2a) was up-regulated (3.4-fold of healthy donors) in the left ventricle of the DCM patients with TTNtv. In contrast, the expression of *MYH6* encoding alpha heavy chain subunit of cardiac myosin, which is also expressed predominantly in atrial tissue, decreased 12.4-fold.

The expression levels of many central genes encoding Z-disk structural proteins were significantly down-regulated in DCM patients with TTNtv compared to healthy donors: *FLNC* (filamin-C; 4.7-fold decrease), *MYOT* (myotilin; 18.1-fold), *PALLD* (palladin; 1.9-fold), *XIRP2* (xin actin-binding repeat containing 2; 6.7-fold), *ZYX* (zyxin; 2.2-fold), *CRYAB* (α -crystallin B chain; 3.2-fold), *MYOZ1* (myozenin-1; 2.3-fold), and *LMCD1* (LIM and cysteine-rich domains 1; 18-fold). *FHL1* (four and a half LIM domains protein 1) and *KLHL40* (kelch-like family member 40) were down-regulated 2.4 and 3.6-fold, respectively. The gene *LMOD2* (leiomodin-2),⁴⁸ an actin-capping and length-regulating protein, was 2.2-fold up-regulated. The expression levels of *MYOM1* and *MYOM2* (myomesin-1 and -2) were 2.1- and 3-fold up-regulated in DCM patients with TTNtv. Myomesin is located in the M-band and links titin to myosin filaments. Overexpression of myomesin was associated with sarcomere damage.⁴⁹ The level of expression of *HSPB1* (heat shock protein beta-1), involved in mechano-transduction,⁵⁰ decreased 3.3-fold. The following extracellular matrix protein genes were up-regulated in DCM patients: *MYOC* (myocilin; 7.5-fold), *FMOD* (fibromodulin; 3.8-fold), *OGN* (osteo-glycin; 3.0-fold), and *SOD3* (extracellular superoxide dismutase [Cu-Zn]; 1.5-fold). The pro-inflammatory protein genes *S100A8* and *S100A9* (calprotectin) were down-regulated 12.5-fold and 15.6-fold, respectively. A marker of endoplasmic reticulum stress, *HSPA5* (heat shock protein family A member 5) was down-regulated 2.2-fold. The full list of the significantly impacted genes is shown in the [Supplementary material online, Table S4](#).

3.2 Protein phosphorylation

We performed Phos-tag gel electrophoresis, in which proteins are separated according to their phosphorylation level, and western blotting to determine the level of Tnl, MyBP-C, and MYL2 phosphorylation in the samples ([Figure 1A and B](#)). Western blots with anti-Tnl antibodies showed three bands corresponding to bis-phosphorylated (at Ser 23 and 24), monophosphorylated and unphosphorylated protein ([Figure 1A](#)). MyBP-C contains three accessible phosphorylated sites (Ser 275, 284, and 304) per molecule.^{22,51} Three or four different migration bands were resolved on western blots with MyBP-C antibodies ([Figure 1A](#)). The intensity of the fourth band (3P) was weak and seen only in the highly phosphorylated control sample NM. All other studied donor heart samples showed only three bands (0P, 1P, and 2P). The level of phosphorylation of Tnl, MyBP-C, and MYL2 was significantly decreased in DCM patients with TTNtv compared to healthy donors ([Figure 1A, B, and D](#)). The level of phosphorylation of Tnl but not MYL2 was also reduced in DCM samples without TTNtv (D12, 0.18 ± 0.02 mol Pi/mol Tnl; D16, 0.74 ± 0.04 mol Pi/mol Tnl; [Figure 1B and D](#)).

We observed a significant negative correlation between Tnl phosphorylation and donor age ([Figure 1C](#)). This suggests that the Tnl phosphorylation level in non-diseased hearts may naturally decline with age. DCM samples with mutations in the *TTN* gene had significantly lower levels of phosphorylation of Tnl: 0.66 ± 0.12 vs. 1.52 ± 0.06 mol Pi/mol Tnl ($P < 0.001$; four patient and 17 donor hearts, respectively; [Figure 1D](#)). The level of phosphorylation of MyBP-C and MYL2 in DCM samples with TTNtv was 0.62 ± 0.18 vs. 1.55 ± 0.08 mol Pi/mol MyBP-C ($P < 0.001$; four patient and 17 donor hearts, respectively; [Figure 1D](#)) and 0.06 ± 0.11 vs. 0.18 ± 0.02 mol Pi/mol MYL2 ($P < 0.05$; four patient and 16 donor hearts, respectively; [Figure 1D](#)).

In the diseased myocardium, the β adrenoceptor is often down-regulated via receptor phosphorylation and β -arrestin binding.⁵² This blunts the response to β -adrenoceptor activation via sympathetic stimulation and thus PKA-induced phosphorylation of contractile proteins. To distinguish the effect of mutation from possible effects caused by dephosphorylation of Tnl and also to understand how phosphorylation of Tnl is associated with heart disease and may change its progression, we manipulated its phosphorylation level in our samples. The PKA catalytic subunit was used to increase the Tnl phosphorylation level in DCM myofibrils. In contrast, λ phosphatase may be used to dephosphorylate Tnl and MyBP-C.^{53,54} Phosphorylation with PKA resulted in fully phosphorylated Tnl (2P per molecule) and MyBP-C (3P per molecule; [Figure 1E](#)). Treatment with λ phosphatase (1000 U/mL, 40 min at 20°C) resulted in fully dephosphorylated Tnl and MyBP-C ([Figure 1E](#)), and a decrease ($\sim 27\%$) in MYL2 phosphorylation ([Figure 1E](#)).

3.3 Myofilament Ca^{2+} sensitivity and Tnl phosphorylation

Myofibril contractility can be described by several parameters: the maximum force of isometric contraction, the Ca^{2+} sensitivity of force production, the rates of force development and relaxation and their modulation by sarcomere length, and Tnl and MyBP-C phosphorylation levels. The maximum force, length dependence of maximal force, kinetics of muscle contraction and relaxation, and passive stiffness have been studied previously in DCM heart samples with truncating mutations.²⁴ Our study focused on the Ca^{2+} sensitivity of force development, its length dependence and the possible functional role of changes in phosphorylation of contractile proteins in the disease. We also verified that myofibrils isolated from an additional DCM sample with TTNtv, D28, had decreased passive stiffness. The Young's modulus was 45.6% lower in D28 compared to donor heart myofibrils, similar to the values found with the other TTNtv DCM samples²⁴ ([Supplementary material online, Figure S2](#)).

Four DCM samples with TTNtv were compared with left ventricular samples of four donor hearts: NM, young adult (23 years old); KN1, middle-aged adult (47 years old), NH (48 years old), and KN2 (61 years old). Tnl and MyBP-C were highly phosphorylated in donor NM (1.80 ± 0.05 mol Pi/mol Tnl and 1.62 ± 0.06 mol Pi/mol MyBP-C) and NH (1.6 ± 0.1 mol Pi/mol Tnl and 1.56 ± 0.11 mol Pi/mol MyBP-C), but not in KN1 (1.18 ± 0.04 mol Pi/mol Tnl and 0.80 ± 0.11 mol Pi/mol MyBP-C). These differentially phosphorylated healthy donor samples were used to distinguish the effect of dephosphorylation of Tnl and MyBP-C regulatory proteins in DCM samples from other effects caused by mutations. The relatively low phosphorylated control sample KN1 was used in functional measurements for the donor-patient comparison. Furthermore, we treated isolated myofibrils with λ phosphatase and PKA to change phosphorylation levels of Tnl and MyBP-C.

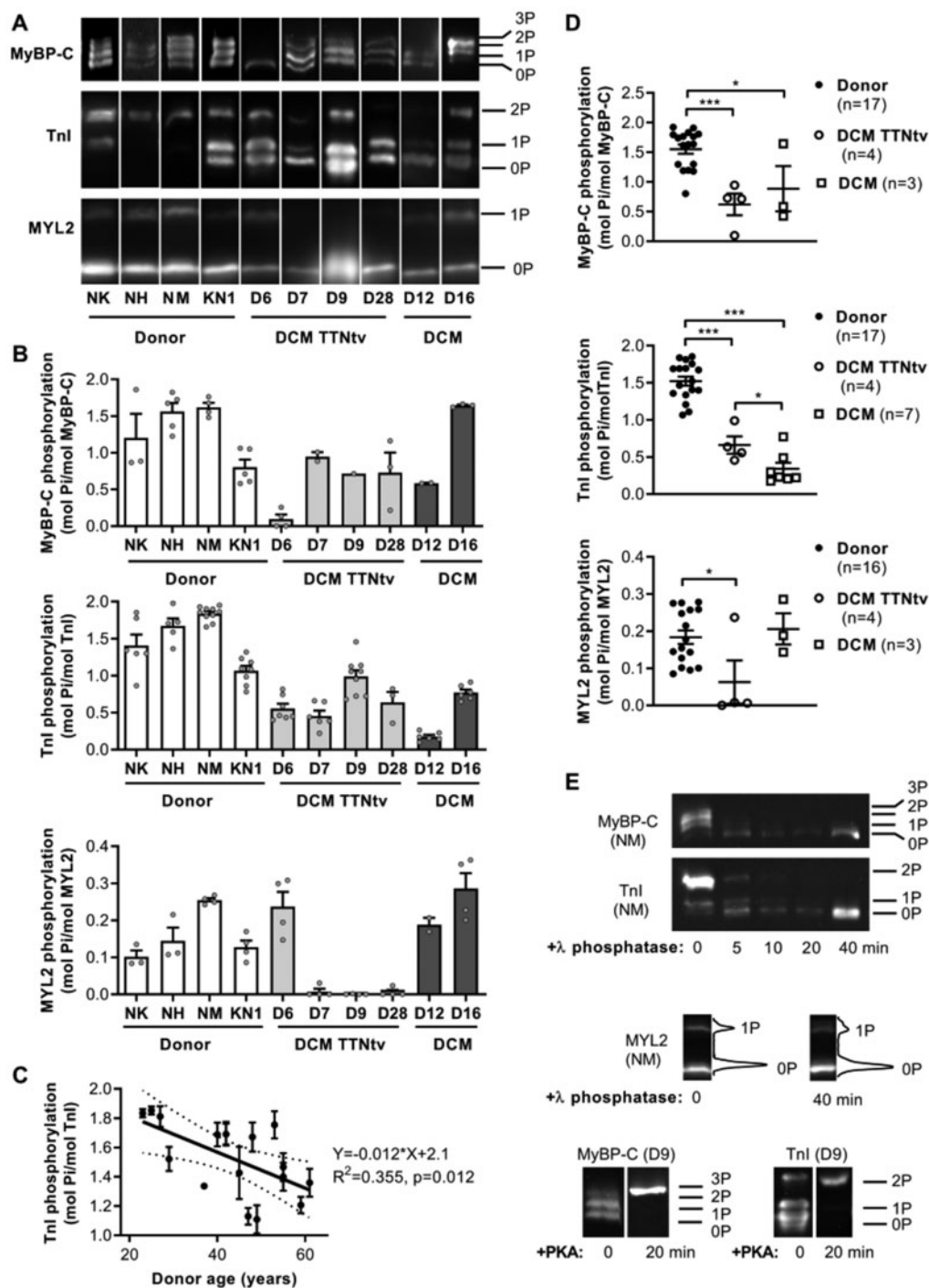


Figure 1 Phosphorylation level of TnI, MyBP-C and MYL2 in the left ventricular myocardium of healthy donor and DCM hearts. (A) Representative western blot image of donor and DCM samples with or without TTNtv. Differently phosphorylated species of TnI, MyBP-C, and MYL2 were separated by Phos-tag SDS page gel followed by Western blotting with anti-TnI, anti-MyBP-C, and anti-MYL2 antibodies. Proteins were separated according to their phosphorylation level: tris-phosphorylated (3P), bis-phosphorylated (2P), monophosphorylated (1P), and unphosphorylated form (0P). Samples are individually plotted to illustrate the range of phosphorylation across donor and DCM heart samples. (B) The densitometric analysis of western blots is shown below each representative western blot. (C) Linear regression analysis of TnI phosphorylation in donors. The scatter plot suggests that TnI phosphorylation declines with donor age. The solid line is a least-squares linear regression line with 95% confidence interval (dotted line). (D) The level of phosphorylation of TnI, MyBP-C, and MYL2 was significantly reduced in DCM patient samples with TTNtv. Phosphorylation levels of TnI in DCM samples 4.032, 4.081, and 3.107 (referred as FA, FC, and FD) have been reported earlier.⁵⁷ Statistical analysis was performed using one-way ANOVA with Fisher's least significant difference test. * $P < 0.05$ and *** $P < 0.001$. (E) Treatment with PKA and λ phosphatase, respectively, increased and decreased the level of phosphorylation of contractile proteins TnI and MyBP-C in myofibrils. λ phosphatase treatment decreased the MYL2 phosphorylation level in NM sample from 25.4% to 18.3%.

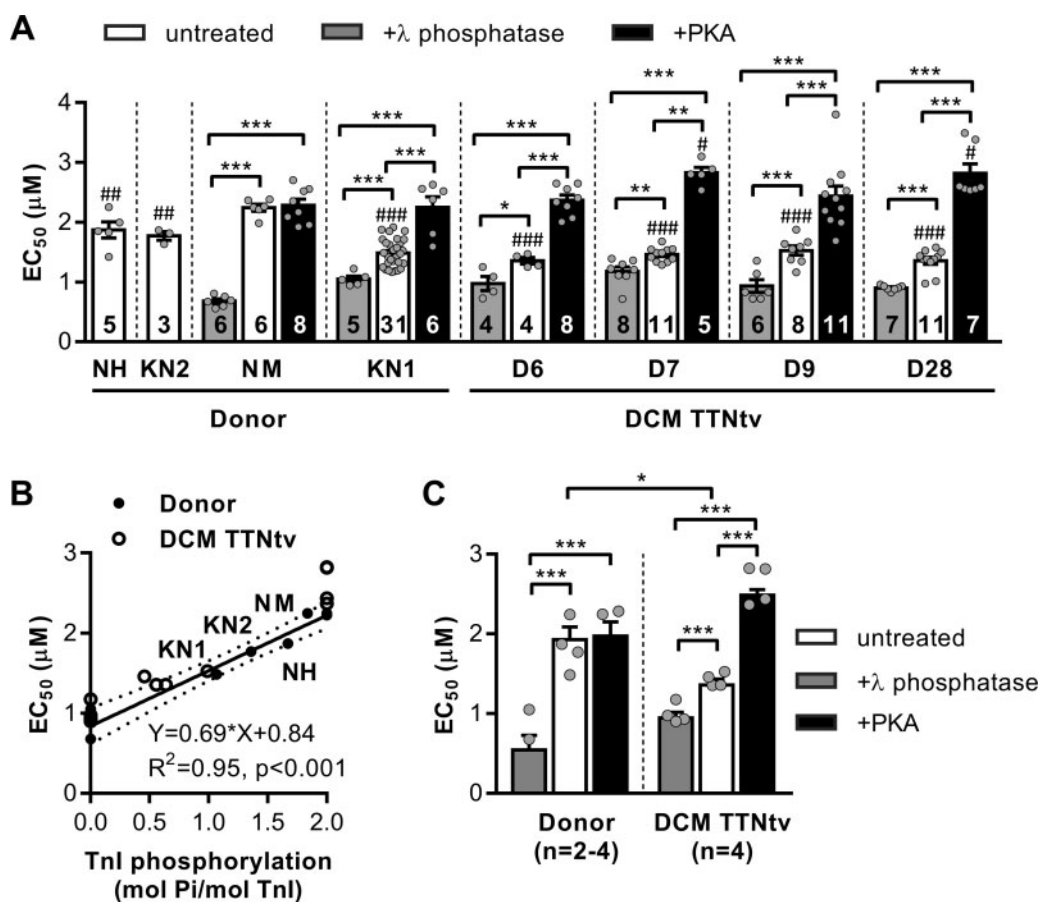


Figure 2 Ca^{2+} sensitivity of force in cardiac myofibrils and its modulation via Tnl phosphorylation. (A) The graph shows the concentrations of Ca^{2+} required for half-maximal force for donor and DCM patient hearts with truncating mutations in the *TTN* gene. Cardiac myofibrils were treated with PKA and λ phosphatase to fully phosphorylate and dephosphorylate Tnl, respectively. Statistical analysis was performed using one-way ANOVA with Fisher's least significant difference test. $^{\#}P < 0.05$, $^{##}P < 0.01$, and $^{###}P < 0.001$ vs. donor NM. $^{*}P < 0.05$, $^{**}P < 0.01$, and $^{***}P < 0.001$ vs. no treatment or other treatment. Numbers on bars indicate number of myofibril samples. (B) Correlation between myofilament Ca^{2+} sensitivity and Tnl phosphorylation. The EC_{50} for Ca^{2+} required for half-maximal force responses in untreated, PKA-, and λ phosphatase-treated cardiac donor myofibrils (closed dots) are plotted against Tnl phosphorylation level. The solid line is a least-squares linear regression line with 95% confidence interval (dotted line). Pearson correlation coefficient $r = 0.91$, $n = 8$ donor hearts (four untreated, two PKA-treated and two λ phosphatase-treated). The open circles are for DCM myofibrils (untreated, PKA-, and λ phosphatase-treated). (C) The EC_{50} values for the combined group of DCMs with TTNtv vs. healthy donors. Sarcomere length was $2.2 \mu m$. Statistical analysis was performed using linear mixed model. Bars show estimated marginal means \pm SE. Grey circles represent mean values of individual heart samples. $^{*}P < 0.05$ and $^{***}P < 0.001$. Measurements were performed at $17^{\circ}C$.

The maximum tension response to different $[Ca^{2+}]$ was fit with the Hill equation to calculate the EC_{50} , $[Ca^{2+}]$ required to reach half-maximal force response. The EC_{50} for donor heart myofibrils was consistent with the Tnl phosphorylation level. Myofibrils with a lower Tnl phosphorylation level had a higher Ca^{2+} sensitivity (lower EC_{50}). The EC_{50} values for donor heart samples NM, NH, KN1, and KN2 were 2.24 ± 0.06 , 1.87 ± 1.14 , 1.48 ± 0.04 , and $1.77 \pm 0.07 \mu mol/L$, respectively (Figure 2A). The Ca^{2+} sensitivities of DCM samples with truncating mutations in the *TTN* gene were significantly higher than those of donor hearts NM (Figure 2A) and NH ($P < 0.038$), but with no significant difference compared to KN1 (Figure 2A). The EC_{50} values for DCM with TTNtv were $1.36 \pm 0.05 \mu mol/L$ for D6, $1.46 \pm 0.04 \mu mol/L$ for D7, $1.53 \pm 0.08 \mu mol/L$ for D9, and $1.36 \pm 0.06 \mu mol/L$ for D28.

The changes in Ca^{2+} sensitivity were coupled to the changes in Tnl phosphorylation level (Figure 2B). Treatment with PKA (fully

phosphorylated Tnl) significantly decreased myofilament Ca^{2+} sensitivity for donor KN1 and DCM with TTNtv samples, and treatment with λ phosphatase (fully unphosphorylated Tnl) significantly increased myofilament Ca^{2+} sensitivity for all samples (Figure 2A and C). The difference between EC_{50} values was not significant between samples of either treatment group when determined at the same phosphorylation level (Figure 2C). However, the EC_{50} value for untreated DCM myofibrils with TTNtv was significantly lower compared to healthy donor heart myofibrils (1.36 ± 0.08 vs. $1.93 \pm 0.16 \mu mol/L$, $P < 0.05$; four patient and four donor hearts; Figure 2C, white bars).

The maximal active tension depended on the sarcomere length, and is a function of overlap between myosin and actin filaments. Treatment with PKA and λ phosphatase did not affect significantly ($P > 0.05$, for all sarcomere lengths) the maximum force of isometric contraction (Supplementary material online, Figure S3) compared to corresponding untreated samples.

The decline in Tnl phosphorylation in DCM hearts is adaptive in the short term as it helps to increase the force of heart contraction. However, such functional tuning can become maladaptive in the long term as it reduces the inotropic reserve of the heart in response to β -adrenergic stimulation.⁵⁵

3.4 Length-dependent activation

Stretching of cardiac myofibril from 2.0 to 2.4 μm significantly decreased the concentration of Ca^{2+} required for half-maximal force production. Control samples showed a shift in force vs. $[\text{Ca}^{2+}]$ curve after changing sarcomere length (Figure 3A, untreated). The shift was greater in the control sample NM ($\Delta\text{EC}_{50} = 0.712 \pm 0.179 \mu\text{mol/L}$) with more highly phosphorylated Tnl than in the sample KN1 ($\Delta\text{EC}_{50} = 0.245 \pm 0.058 \mu\text{mol/L}$; Figure 3A). The mean value of ΔEC_{50} for healthy donor heart myofibrils was $0.583 \pm 0.164 \mu\text{mol/L}$ ($n = 5$ hearts, linear mixed model analysis; Figure 3C). In contrast, length dependence of Ca^{2+} sensitivity was not seen in four DCM samples with TTNtv ($\Delta\text{EC}_{50} = -0.037 \pm 0.051 \mu\text{mol/L}$, $n = 4$ hearts; Figure 3C). Importantly, we showed that the length dependence of EC_{50} was preserved in control sample KN1 (Figure 3A, white bars), with a low phosphorylation level of both Tnl ($1.18 \pm 0.04 \text{ mol Pi/mol Tnl}$) and MyBP-C ($0.80 \pm 0.11 \text{ mol Pi/mol MyBP-C}$). Moreover, the shift in EC_{50} was also observed in DCM samples D12 and D16 with a lower level of Tnl phosphorylation but without TTNtv ($\Delta\text{EC}_{50} = 0.403 \pm 0.089 \mu\text{mol/L}$, $n = 2$ hearts; Figure 3C).

To determine whether the decrease in phosphorylation can affect length-dependent activation, we used samples with different levels of phosphorylation of Tnl: native and fully phosphorylated by PKA. Decreased level of Tnl phosphorylation in heart failure samples correlates with a decreased length-dependent activation.⁵⁶ PKA treatment restored length-dependent changes in EC_{50} in DCM with TTNtv ($\Delta\text{EC}_{50} = 0.78 \pm 0.12 \mu\text{mol/L}$, $n = 4$ hearts; Figure 3C, black bars). This value is similar to the values we found for the highly phosphorylated control NM ($\Delta\text{EC}_{50} = 0.71 \pm 0.18 \mu\text{mol/L}$ for untreated NM and $\Delta\text{EC}_{50} = 0.79 \pm 0.16 \mu\text{mol/L}$ for PKA-treated NM; Figure 3A). However, in the case of DCM with TTNtv, length-dependent activation was not present in sample D9, with phosphorylation levels of Tnl and MyBP-C similar to control KN1, as well as in other samples with TTNtv (Figure 3B, white bars). Also, length-dependent activation was present in samples D12 and D16 (Figure 3A), where the phosphorylation level of Tnl was lowest.

We concluded that a certain level of phosphorylation of Tnl is essential, but not enough for normal length-dependent activation. TTN mutations led to decreased length-dependent activation independently of the dephosphorylation of Tnl and MyBP-C. Dephosphorylation of regulatory proteins during disease progression and ageing can only cause further impairment of both length-dependent activation and the rate of contraction.

4. Discussion

Phosphorylation levels of Tnl and MyBP-C are usually reduced in cardiomyopathies.^{22,56–59} The reason for this is that diseased myocardium β adrenoceptors are often down-regulated via receptor phosphorylation and β -arrestin binding.⁵² Phosphorylation levels of Tnl and MyBP-C are decreased in idiopathic DCM^{58,59} and normal in a number of human DCM samples with mutations in thin-filament protein genes (*TNNI3*, *TNNI2*, *TNNC1*),^{59,60} but reduced in DCM samples with TTNtv (Figure 1D). Moreover, phosphorylation of MYL2 was significantly reduced in DCM with TTNtv (Figure 1D); three of four studied samples

were virtually unphosphorylated (Figure 1B). This is in contrast to idiopathic DCM, not associated with TTNtv, which showed MYL2 phosphorylation level comparable to donor hearts.^{61,62}

Higher Ca^{2+} sensitivity in DCM muscles with mutations in TTN (Figure 2C) was associated with a reduced phosphorylation level of Tnl compared to donor hearts (Figure 1D). The Ca^{2+} sensitivity in DCM myofibrils was modulated via Tnl phosphorylation (Figure 2B). Myofibrils with higher levels of phosphorylation had faster cross-bridge kinetics, higher rates of contraction (k_{ACT} ; Supplementary material online, Figure S5B), and relaxation (lower t_{LIN} and higher k_{REL} ; Supplementary material online, Figure S5C and E). Interestingly, our data suggest that Tnl phosphorylation level may naturally decline with age (Figure 1C).

Length-dependent activation is the basis for the Frank–Starling law, which states that the force of contraction increases with diastolic volume and therefore with the length of the cardiomyocytes.³⁴ However, the mechanism of length-dependent activation is still not well understood.³⁵ The length-dependent shift in calcium sensitivity was absent in DCM myofibrils with TTN-truncating mutations (Figure 3B and C, white bars).

DCM mutations in TTN lead to a totally blunted length-dependent shift in the Ca^{2+} sensitivity of contraction and therefore impaired Frank–Starling mechanism. This provides a distinct mechanism of TTNtv, compared to DCM caused by other factors. In our study, we clearly revealed no difference in ΔEC_{50} (Figure 3D), or ratio of EC_{50} (Supplementary material online, Figure S6) values measured at short and long sarcomere lengths in DCM samples with TTNtv, compared to donor hearts. We would like to point out that the ratio of EC_{50} values measured at short and long sarcomere lengths is a more appropriate parameter to evaluate changes in calcium sensitivity. The EC_{50} mean ratio for DCM with TTNtv was 0.98 ± 0.03 ($n = 4$ hearts; Supplementary material online, Figure S6); otherwise the ratio for donor hearts was much higher, at 1.44 ± 0.07 ($n = 5$ hearts; Supplementary material online, Figure S6). In other studies, length-dependent activation (ΔEC_{50}) has been found unchanged in ischaemic cardiomyopathy and not significantly decreased in other DCM samples, and the EC_{50} ratio between the donor and DCM patient cardiomyocytes not different.^{59,63,64} PKA effectively restored length-dependent changes in myofilament Ca^{2+} sensitivity in DCM hearts with TTNtv (Figure 3D).

We cannot exclude that phosphorylation of Tnl modulates the length-dependent changes in Ca^{2+} sensitivity.⁶⁵ However, the low level of Tnl phosphorylation in DCM TTNtv myofibrils still does not fully explain the loss of response to stretch. Indeed, the stretch-activated Ca^{2+} sensitization was preserved in the donor heart sample KN1, with the low level of phosphorylation of both Tnl and MyBP-C, and in DCM samples D12 and D16 (Figure 3A). We propose that a certain level of Tnl phosphorylation is required for normal stretch-activated Ca^{2+} sensitization, but this phosphorylation threshold is increased in DCM muscle with TTNtv. Therefore, a reduced Tnl phosphorylation in TTNtv patients is not sufficient for normal length-dependent activation. PKA phosphorylation may thus compensate for the loss of function. The decrease in phosphorylation occurring during ageing and disease progression worsens heart functionality and can lead further to heart failure.

The possible factors that modulate the passive stiffness of myofibrils (selective phosphorylation of titin and its alternative splicing) are still under investigation.²⁶ PKA phosphorylates titin in the N2B domain (Ser 4065 and 4185) and decreases passive stiffness.³¹ Interestingly, decreased passive stiffness was associated with decreased length-dependent activation.⁶⁶ It may indirectly suggest that phosphorylation of titin by PKA is not the factor increasing length-dependent activation. However, there are not enough studies on the role of titin

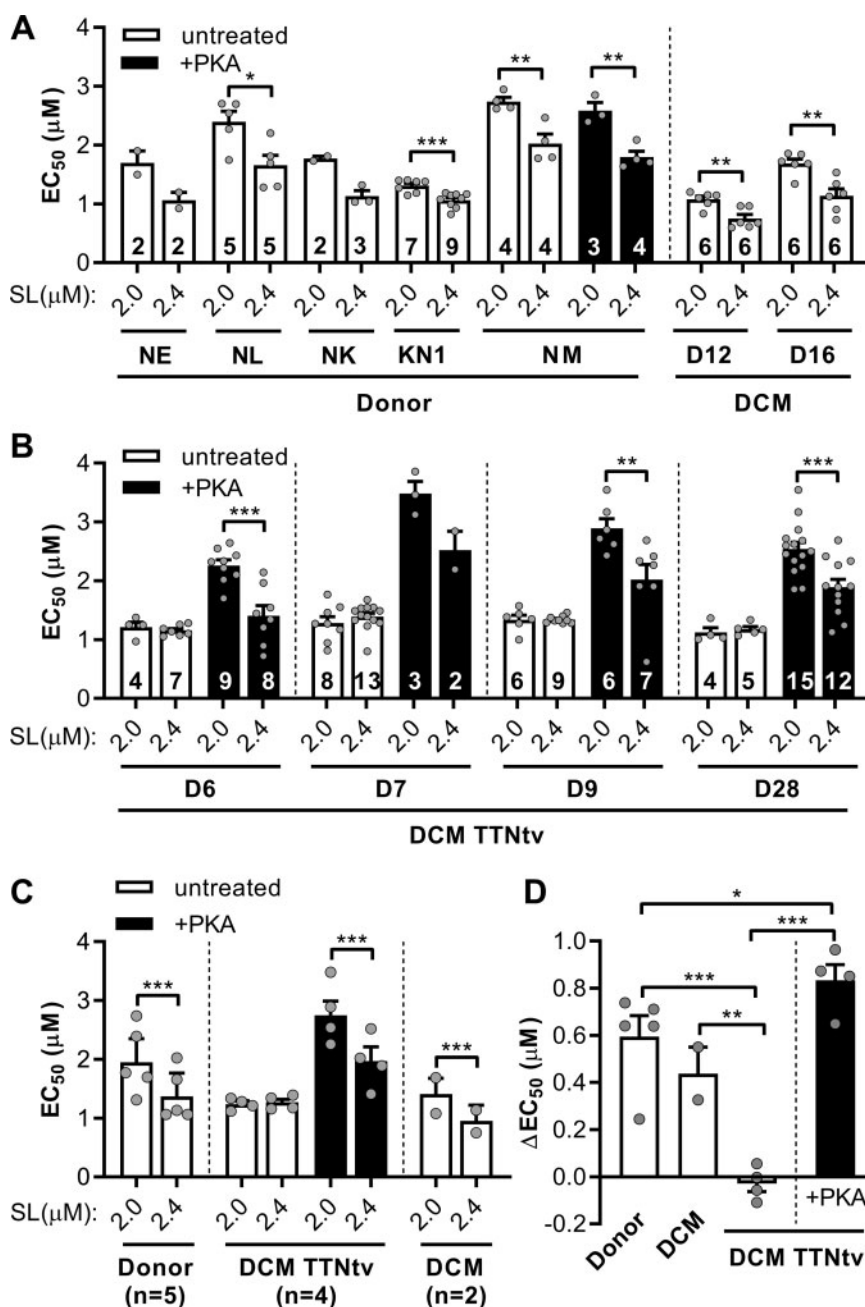


Figure 3 Length dependence of the Ca^{2+} sensitivity of force. The maximum force was measured at different concentrations of Ca^{2+} and the EC_{50} required for the half-maximal activation was calculated. The measurements were performed at short (2.0 μm) and long (2.4 μm) sarcomere lengths (SL). (A) The calcium sensitivity of force (EC_{50}) in donor heart myofibrils and DCM myofibrils without TTNtv. A significant shift in EC_{50} was observed both in low- and high-phosphorylated healthy donor heart and DCM without TTNtv samples. (B) Mutations in titin abolished the length-dependent changes in EC_{50} . The changes in EC_{50} by stretch were restored by PKA-induced phosphorylation. Statistical analysis was performed using Student's *t*-test or the Mann-Whitney *U* test. * $P < 0.05$, ** $P < 0.01$, and *** $P < 0.001$. Numbers on bars indicate number of myofibril samples. (C) Statistics for the combined group of DCMs and healthy donors. Statistical analysis was performed using linear mixed model. Bars show estimated marginal means \pm SE. Grey circles represent mean values of individual heart samples. (D) The difference between the EC_{50} values measured at 2.0 μm and 2.4 μm . Statistical analysis was performed using one-way ANOVA with Fisher's least significant difference test. Grey circles represent mean ΔEC_{50} values of individual heart samples. Measurements were performed at 17°C.

phosphorylation in length-dependent activation. Previously, we showed that DCM with TTNtv and donor samples have similar titin protein phosphorylation levels, long to short titin isoform ratios (N2BA/N2B)

and no expression of truncated titin protein variants,²⁴ which is consistent with earlier studies.^{15,33} N2BA/N2B ratios are found unchanged in familial DCM²⁴ but increased in patients with idiopathic DCM.^{24,25,64,67}

Mutation in the *RBM20* gene caused decreased passive stiffness of titin as well as length-dependent activation.⁶⁴

We consider a complex interplay between titin passive stiffness, stretch-induced structural changes in myosin, troponin, myosin-binding protein C,⁶⁸ and the phosphorylation status of Tnl and MyBP-C on the length-dependent changes in Ca^{2+} -sensitivity.

To understand further the mechanism of influence of titin mutations on length-dependence activation, we performed mRNA sequencing of four DCM samples with truncation mutations in the *TTN* gene. We did not find a significantly different expression of *TTN* mRNA compared to healthy donors. *TTN* exon usage and splicing were also very similar (Supplementary material online, Figure S1 and Table S3).

Nevertheless, mutations in the *TTN* gene may have a significant impact on the earlier stages of heart development, e.g. pre- and postnatal, and lead to disruption of the expression of proteins interacting with titin in the adult heart. Also, cardiovascular stress may play a role in the clinical manifestation of DCM in this group of patients. Increased intracellular Ca^{2+} concentration, cellular, and endoplasmic reticulum stress inhibit nonsense-mediated mRNA decay.⁶⁹ This increases expression of truncated proteins and, in our case, stress may induce temporary expression of truncated titin variants at early stages of the disease.

We found a strong down-regulation of mRNA expression of numerous cytoskeletal proteins associated with the Z-disk. This may not be a coincidence and indeed may have important functional consequences. Many of these genes encoding Z-disk proteins are associated with the so-called myofibrillar myopathies^{70–72} and DCM.¹² The Z-disk is important for mechanical stability, mechanotransduction, and signalling.⁷³ Both actin and titin filaments are embedded in the Z-disk of sarcomeres via TCAP, α -actinin, and other proteins.^{23,74,75} It implies that Z-disk proteins might modulate myofibril contractility. The decreased expression of Z-disk proteins may lead to a disruption of the Z-disk structure. Therefore, we believe that loss of Z-disk integrity may explain the observed decrease in myofibril passive stiffness and length-dependent activation. Indeed, we found that the length-dependent changes in Ca^{2+} sensitivity observed in healthy donor heart samples were absent in heart samples with mutations in the *TTN*. Thus, titin contributes to the Frank–Starling mechanism not only as a passive elastic component but also as an active regulator of actin–myosin interaction (Figure 5).

We measured ATPase activity in thin muscle strips under relaxing conditions (basal ATPase activity) and then at different concentrations of Ca^{2+} during isometric contraction. We cannot draw a general conclusion for this study because of the small number of samples used, but these results should stimulate further investigation in this area. Mutations in *TTN* did not change the tension cost of force generation (Supplementary material online, Figure S7D), but significantly decreased the maximal ATP consumption rate (Figure 4B) and increased basal ATPase activity of myosin (Figure 4A). Similarly, DCM-associated mutations in *MYH7* also decrease myosin actin-activated ATPase activity.⁷⁶ In contrast, a hypertrophic cardiomyopathy mutation in cardiac troponin T, K280N, increases the energy cost of tension generation but does not affect resting ATP activity.⁷⁷ Basal myosin ATPase can also be significantly increased, as shown in mouse models of HCM.⁷⁸ Basal ATPase activity has been found similar in ventricular and atrial muscle strips.⁷⁹ Therefore, it is unlikely that the increased expression of the atrial

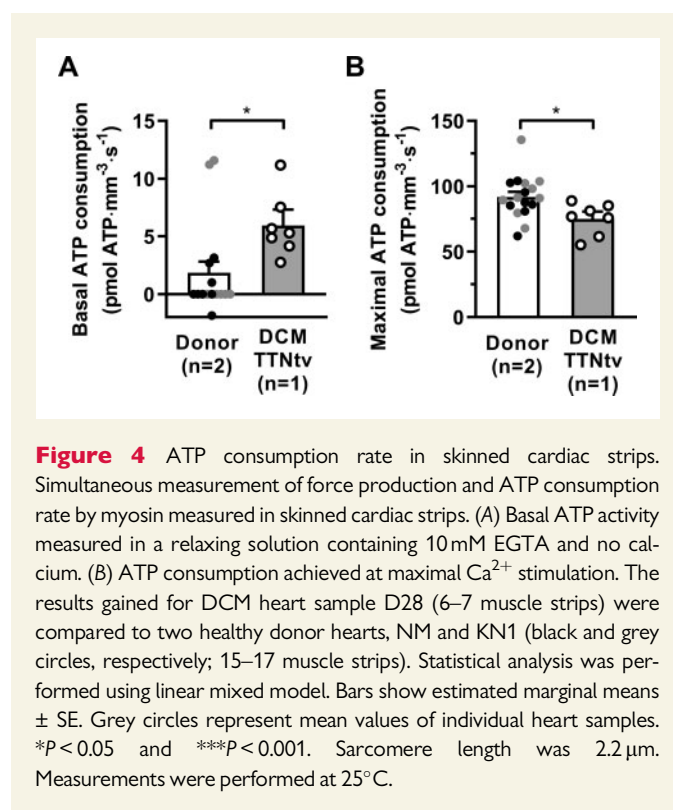


Figure 4 ATP consumption rate in skinned cardiac strips. Simultaneous measurement of force production and ATP consumption rate by myosin measured in skinned cardiac strips. (A) Basal ATP activity measured in a relaxing solution containing 10 mM EGTA and no calcium. (B) ATP consumption achieved at maximal Ca^{2+} stimulation. The results gained for DCM heart sample D28 (6–7 muscle strips) were compared to two healthy donor hearts, NM and KN1 (black and grey circles, respectively; 15–17 muscle strips). Statistical analysis was performed using linear mixed model. Bars show estimated marginal means ± SE. Grey circles represent mean values of individual heart samples. *P < 0.05 and ***P < 0.001. Sarcomere length was 2.2 μm . Measurements were performed at 25°C.

isoform of myosin regulatory light chain 2 is associated with the increased basal ATP activity of myosin in DCM samples with TTNtv. Increased basal myosin ATPase could be related to destabilization of the super-relaxed state. The ratio of systolic to diastolic duration in the adult human heart is ~0.6 and 0.9 at rest and during exercise, respectively.⁸⁰ The ratio of basal to maximal ATP consumption in DCM cardiac strips (Figure 4A and B) was 0.08. Therefore, we can assume that at rest, ATP use by myosin during diastole in the myocardium of DCM patients with TTNtv can be more than 12% of total ATP consumption. This is 3.6 times higher compared to the healthy myocardium (~3%).

In conclusion, the results demonstrate that decreased length-dependent activation induced by mutations in the structural protein titin could be one of the most important factors in DCM pathogenesis. The increase in Ca^{2+} sensitivity, due to Tnl phosphorylation level decreases, is a secondary factor that is initially adaptive but then becomes maladaptive. The decrease in length-dependent activation and reduced passive stiffness impair the Frank–Starling mechanism. Moreover, we can propose that DCM-truncating mutations in *TTN* may increase consumption of ATP during diastole that may lead to ATP depletion observed in DCM myocardium (35%)⁸¹ and cardiomyocyte wasting. However, the limited number of studied DCM samples with TTNtv will require follow-up work to support our conclusions in a larger cohort of patients with TTNtv.

Supplementary material

Supplementary material is available at *Cardiovascular Research* online.

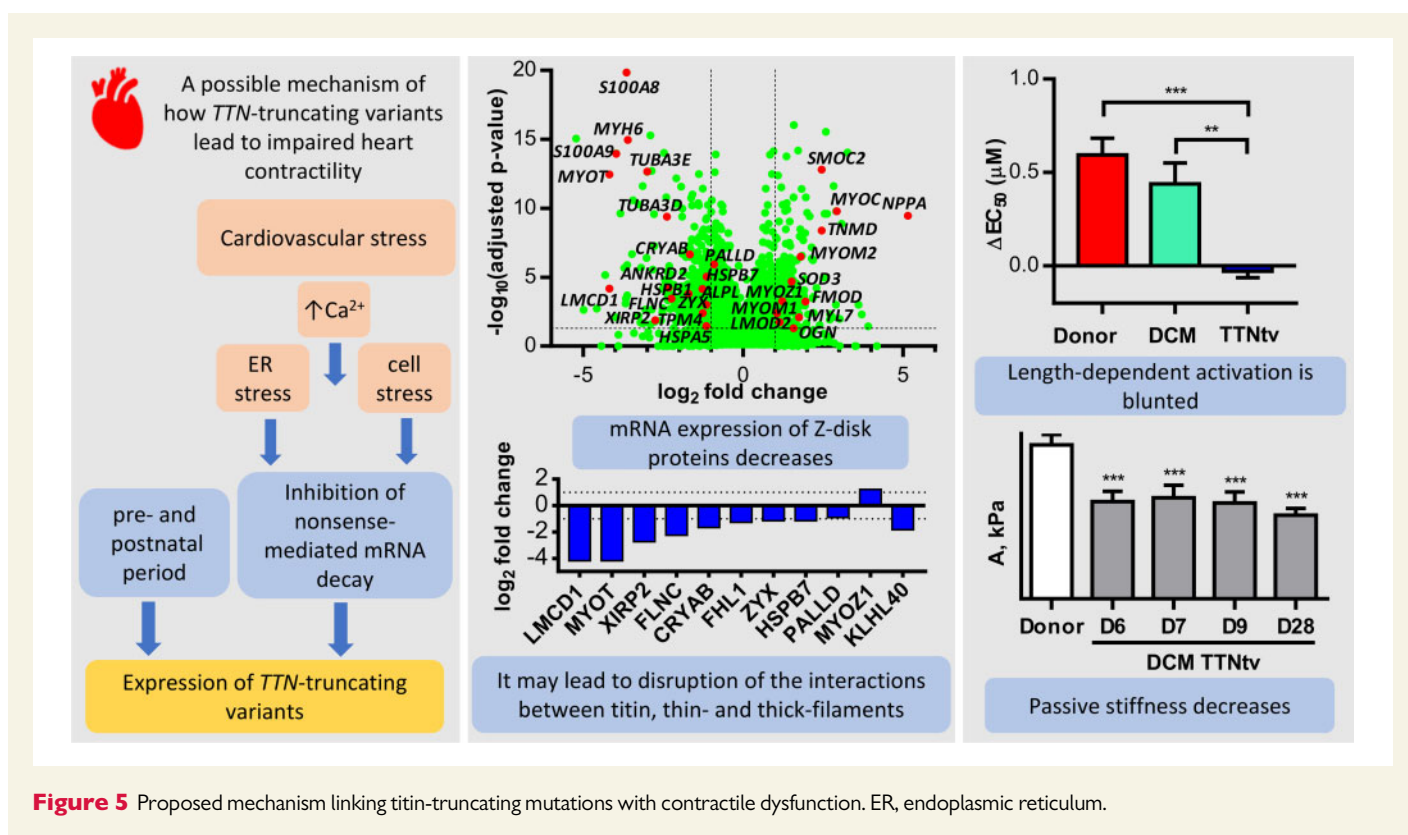


Figure 5 Proposed mechanism linking titin-truncating mutations with contractile dysfunction. ER, endoplasmic reticulum.

Author contributions

P.G.V., N.N.V., and P.d.T. conceived the study or contributed to the experimental design. P.G.V., N.N.V., and W.C. performed experiments and data analysis. A.L., S.L., C.G.d.R., C.A.B., M.G., K.S.C., and S.B.M. provided human heart samples. P.G.V. and N.N.V. wrote the manuscript with help from C.G.d.R. All authors discussed the results and commented on the manuscript. All authors approved the final version of the manuscript.

Conflict of interest: none declared.

Funding

The work was supported by a grant from the British Heart Foundation [PG/17/5/32705 to P.G.V. and S.B.M.]; the National Institutes of Health grant [HL-PO1 HL62426 to P.d.T.]; the Fondation Leducq [17CVD04 to M.H.Y.]; and by the Magdi Yacoub Institute [Charity number 1082750].

Data availability

The data underlying this article are available in the article and in its online [supplementary material](#). The raw mRNA sequencing data cannot be made publicly available due to ethical restrictions.

Acknowledgements

We thank the patients and staff of St. Vincent's Hospital Darlinghurst Australia and the University of Kentucky Hospital, Lexington, KY, USA.

References

- Swedberg K, Cleland J, Dargie H, Drexler H, Follath F, Komajda M, Tavazzi L, Smiseth OA, Gavazzi A, Haverich A, Hoes A, Jaarsma T, Korewicki J, Lévy S, Linde C, Lopez-Sendon J-L, Nieminen MS, Piérard L, Remme WJ. Guidelines for the diagnosis and treatment of chronic heart failure: executive summary (update 2005): the task force for the diagnosis and treatment of chronic heart failure of the European Society of Cardiology. *Eur Heart J* 2005;**26**:1115–1140.
- Taylor CJ, Ordonez-Mena JM, Roalke AK, Lay-Flurrie S, Jones NR, Marshall T, Hobbs FDR. Trends in survival after a diagnosis of heart failure in the United Kingdom 2000–2017: population based cohort study. *Br Med J* 2019;**364**:i223.
- Conrad N, Judge A, Tran J, Mohseni H, Hedgecott D, Crespiello AP, Allison M, Hemingway H, Cleland JG, McMurray JJV, Rahimi K. Temporal trends and patterns in heart failure incidence: a population-based study of 4 million individuals. *Lancet* 2018;**391**:572–580.
- Benjamin EJ, Muntner P, Alonso A, Bittencourt MS, Callaway CW, Carson AP, Chamberlain AM, Chang AR, Cheng S, Das SR, Delling FN, Djousse L, Elkind MSV, Ferguson JF, Fornage M, Jordan LC, Khan SS, Kissela BM, Knutson KL, Kwan TW, Lackland DT, Lewis TT, Lichtman JH, Longenecker CT, Loop MS, Lutsey PL, Martin SS, Matsushita K, Moran AE, Mussolino ME, O'Flaherty M, Pandey A, Perak AM, Rosamond WD, Roth GA, Sampson UKA, Satou GM, Schroeder EB, Shah SH, Spartano NL, Stokes A, Tirschwell DL, Tsao CW, Turakhia MP, VanWagner LB, Wilkins JT, Wong SS, Virani SS; On behalf of the American Heart Association Council on Epidemiology and Prevention Statistics Committee and Stroke Statistics Subcommittee. Heart disease and stroke statistics-2019 update: a report from the American Heart Association. *Circulation* 2019;**139**:e56–e528.
- Aragam KG, Chaffin M, Levinson RT, McDermott G, Choi SH, Shoemaker MB, Haas ME, Weng L-C, Lindsay ME, Smith JG, Newton-Cheh C, Roden DM, London B, Wells QS, Ellinor PT, Kathiresan S, Lubitz SA, Bloom HL, Dudley SC, Shalaby AA, Weiss R, Gutmann R, Saba S; for the GRADE Investigators. Phenotypic refinement of heart failure in a National Biobank facilitates genetic discovery. *Circulation* 2019;**139**:489–501.
- Baldasseroni S, De Biase L, Fresco C, Marchionni N, Marini M, Masotti G, Orsini G, Porcu M, Pozzar F, Scherillo M, Maggioni AP, Failure I. Cumulative effect of complete left bundle-branch block and chronic atrial fibrillation on 1-year mortality and hospitalization in patients with congestive heart failure. A report from the Italian Network on Congestive Heart Failure (in-CHF database). *Eur Heart J* 2002;**23**:1692–1698.
- Shore S, Grau-Sepulveda MV, Bhatt DL, Heidenreich PA, Eapen ZJ, Hernandez AF, Yancy CW, Fonarow GC. Characteristics, treatments, and outcomes of hospitalized heart failure patients stratified by etiologies of cardiomyopathy. *J Am Coll Cardiol* 2015;**3**:906–916.
- Tromp J, Tay WT, Ouwerkerk W, Teng TK, Yap J, MacDonald MR, Leineweber K, McMurray JJV, Zile MR, Anand IS, Richards AMR, Lam CSP, Authors A; ASIAN-HF authors. Multimorbidity in patients with heart failure from 11 Asian regions: a prospective cohort study using the ASIAN-HF registry. *PLoS Med* 2018;**15**:e1002541.

9. Schultheiss HP, Fairweather D, Caforio ALP, Escher F, Hershberger RE, Lipshultz SE, Liu PP, Matsumori A, Mazzanti A, McMurray J, Priori SG. Dilated cardiomyopathy. *Nat Rev Dis Primers* 2019;**5**:32.
10. Bozkurt B, Colvin M, Cook J, Cooper LT, Deswal A, Fonarow GC, Francis GS, Lenihan D, Lewis EF, McNamara DM, Pahl E, Vasan RS, Ramasubbu K, Rasmussen K, Towbin JA, Yancy C. Current diagnostic and treatment strategies for specific dilated cardiomyopathies: a scientific statement from the American Heart Association. *Circulation* 2016;**134**:e579–e646.
11. McNally EM, Mestroni L. Dilated cardiomyopathy: genetic determinants and mechanisms. *Circ Res* 2017;**121**:731–748.
12. Burke MA, Cook SA, Seidman JG, Seidman CE. Clinical and mechanistic insights into the genetics of cardiomyopathy. *J Am Coll Cardiol* 2016;**68**:2871–2886.
13. Herman DS, Lam L, Taylor MR, Wang L, Teekakirikul P, Christodoulou D, Conner L, DePalma SR, McDonough B, Sparks E, Teodorescu DL, Cirino AL, Banner NR, Pennell DJ, Graw S, Merlo M, Di Lenarda A, Sinagra G, Bos JM, Ackerman MJ, Mitchell RN, Murry CE, Lakdawala NK, Ho CY, Barton PJ, Cook SA, Mestroni L, Seidman JG, Seidman CE. Truncations of titin causing dilated cardiomyopathy. *N Engl J Med* 2012;**366**:619–628.
14. Mazzarotto F, Tayal U, Buchan RJ, Midwinter W, Wilk A, Whiffin N, Govind R, Mazaika E, de Marvao A, Dawes TJW, Felkin LE, Ahmad M, Theotokis PI, Edwards E, Ing AY, Thomson KL, Chan LLH, Sim D, Baksi AJ, Pantazis A, Roberts AM, Watkins H, Funke B, O'Regan DP, Olivetto I, Barton PJR, Prasad SK, Cook SA, Ware JS, Walsh R. Reevaluating the genetic contribution of monogenic dilated cardiomyopathy. *Circulation* 2020;**141**:387–398.
15. Roberts AM, Ware JS, Herman DS, Schafer S, Baksi J, Bick AG, Buchan RJ, Walsh R, John S, Wilkinson S, Mazzarotto F, Felkin LE, Gong S, L MacArthur JA, Cunningham F, Flannick J, Gabriel SB, Altshuler DM, Macdonald PS, Heine M, Keogh AM, Hayward CS, Banner NR, Pennell DJ, O'Regan DP, San TR, de Marvao A, W, Dawes TJ, Gulati A, Birks EJ, Yacoub MH, Radke M, Gotthardt M, Wilson JG, O'Donnell CJ, Prasad SK, R. Barton PJ, Fatkin D, Hubner N, Seidman JG, Seidman CE, Cook SA. Integrated allelic, transcriptional, and phenomic dissection of the cardiac effects of titin truncations in health and disease. *Sci Transl Med* 2015;**7**:270a6.
16. Garcia-Pavia P, Kim Y, Restrepo-Cordoba MA, Lunde IG, Wakimoto H, Smith AM, Toepfer CN, Getz K, Gorham J, Patel P, Ito K, Willcox JA, Arany Z, Li J, Owens AT, Govind R, Nuñez B, Mazaika E, Bayes-Genis A, Walsh R, Finkelman B, Lupón J, Whiffin N, Serrano I, Midwinter W, Wilk A, Bardaji A, Ingold N, Buchan R, Tayal U, Pascual-Figal DA, de Marvao A, Ahmad M, Garcia-Pinilla JM, Pantazis A, Dominguez F, John Baksi A, O'Regan DP, Rosen SD, Prasad SK, Lara-Pezzi E, Provencio M, Lyon AR, Alonso-Pulpon L, Cook SA, DePalma SR, Barton PJR, Aplenc R, Seidman JG, Ky B, Ware JS, Seidman CE. Genetic variants associated with cancer therapy-induced cardiomyopathy. *Circulation* 2019;**140**:31–41.
17. Gammill HS, Chettier R, Brewer A, Roberts JM, Shree R, Tsigas E, Ward K. Cardiomyopathy and preeclampsia. *Circulation* 2018;**138**:2359–2366.
18. Linschoten M, Teske AJ, Baas AF, Vink A, Dooijes D, Baars HF, Asselbergs FW. Truncating titin (TTN) variants in chemotherapy-induced cardiomyopathy. *J Cardiac Fail* 2017;**23**:476–479.
19. Ware JS, Amor-Salamanca A, Tayal U, Govind R, Serrano I, Salazar-Mendiguchía J, García-Pinilla JM, Pascual-Figal DA, Nuñez J, Guzzo-Merello G, Gonzalez-Vioque E, Bardaji A, Manito N, López-Garrido MA, Padron-Barthe L, Edwards E, Whiffin N, Walsh R, Buchan RJ, Midwinter W, Wilk A, Prasad S, Pantazis A, Baski J, O'Regan DP, Alonso-Pulpon L, Cook SA, Lara-Pezzi E, Barton PJ, Garcia-Pavia P. Genetic etiology for alcohol-induced cardiac toxicity. *J Am Coll Cardiol* 2018;**71**:2293–2302.
20. Solaro RJ, Kobayashi T. Protein phosphorylation and signal transduction in cardiac thin filaments. *J Biol Chem* 2011;**286**:9935–9940.
21. Barefield D, Sadayappan S. Phosphorylation and function of cardiac myosin binding protein-C in health and disease. *J Mol Cell Cardiol* 2010;**48**:866–875.
22. Copeland O, Sadayappan S, Messer AE, Steinen GJ, van der Velden J, Marston SB. Analysis of cardiac myosin binding protein-C phosphorylation in human heart muscle. *J Mol Cell Cardiol* 2010;**49**:1003–1011.
23. Linke WA. Sense and stretchability: the role of titin and titin-associated proteins in myocardial stress-sensing and mechanical dysfunction. *Cardiovasc Res* 2008;**77**:637–648.
24. Vikhorev PG, Smoktunowicz N, Munster AB, Copeland O, Kostin S, Montgiraud C, Messer AE, Toliat MR, Li A, dos Remedios CG, Lal S, Blair CA, Campbell KS, Guglin M, Richter M, Knoll R, Marston SB. Abnormal contractility in human heart myofibrils from patients with dilated cardiomyopathy due to mutations in TTN and contractile protein genes. *Sci Rep* 2017;**7**:14829.
25. Makarenko I, Opitz CA, Leake MC, Neagoe C, Kulke M, Gwathmey JK, del Monte F, Hajjar RJ, Linke WA. Passive stiffness changes caused by upregulation of compliant titin isoforms in human dilated cardiomyopathy hearts. *Circ Res* 2004;**95**:708–716.
26. Koser F, Loescher C, Linke WA. Posttranslational modifications of titin from cardiac muscle: how, where, and what for? *FEBS J* 2019;**286**:2240–2260.
27. Linke WA, Hamdani N. Gigantic business: titin properties and function through thick and thin. *Circ Res* 2014;**114**:1052–1068.
28. Brauch KM, Karst ML, Herron KJ, de Andrade M, Pellikka PA, Rodeheffer RJ, Michels VV, Olson TM. Mutations in ribonucleic acid binding protein gene cause familial dilated cardiomyopathy. *J Am Coll Cardiol* 2009;**54**:930–941.
29. Rexiati M, Sun M, Guo W. Muscle-specific mis-splicing and heart disease exemplified by RBM20. *Genes (Basel)* 2018;**9**:18.
30. Guo W, Schafer S, Greaser ML, Radke MH, Liss M, Govindarajan T, Maatz H, Schulz H, Li S, Parrish AM, Dauksaite V, Vakeel P, Klaassen S, Gerull B, Thierfelder L, Regitz-Zagrosek V, Hacker TA, Saue KW, Dec GW, Elinor PT, MacRae CA, Spallek B, Fischer R, Perrot A, Ozelik C, Saar K, Hubner N, Gotthardt M, RBM20, a gene for hereditary cardiomyopathy, regulates titin splicing. *Nat Med* 2012;**18**:766–773.
31. Kötter S, Gout L, Von Frieling-Salewski M, Müller AE, Helling S, Marcus K, Dos Remedios C, Linke WA, Krüger M. Differential changes in titin domain phosphorylation increase myofilament stiffness in failing human hearts. *Cardiovasc Res* 2013;**99**:648–656.
32. Krüger M, Kötter S, Grützner A, Lang P, Andresen C, Redfield MM, Butt E, dos Remedios CG, Linke WA. Protein kinase G modulates human myocardial passive stiffness by phosphorylation of the titin springs. *Circ Res* 2009;**104**:87–94.
33. Gammill HS, Michely B, Krohne C, Heuser A, Erdmann B, Klaassen S, Hudson B, Magarin M, Kirchner F, Todiras M, Granzier H, Labeit S, Thierfelder L, Gerull B. Stress-induced dilated cardiomyopathy in a knock-in mouse model mimicking human titin-based disease. *J Mol Cell Cardiol* 2009;**47**:352–358.
34. Katz AM. Ernest Henry Starling, his predecessors, and the "Law of the Heart". *Circulation* 2002;**106**:2986–2992.
35. Sequeira V, van der Velden J. Historical perspective on heart function: the Frank-Starling Law. *Biophys Rev* 2015;**7**:421–447.
36. McNamara JW, Li A, Dos Remedios CG, Cooke R. The role of super-relaxed myosin in skeletal and cardiac muscle. *Biophys Rev* 2015;**7**:5–14.
37. Kampourakis T, Sun YB, Irving M. Myosin light chain phosphorylation enhances contraction of heart muscle via structural changes in both thick and thin filaments. *Proc Natl Acad Sci USA* 2016;**113**:E3039–E3047.
38. McNamara JW, Li A, Lal S, Bos JM, Harris SP, van der Velden J, Ackerman MJ, Cooke R, dos Remedios CG. MYBPC3 mutations are associated with a reduced super-relaxed state in patients with hypertrophic cardiomyopathy. *PLoS One* 2017;**12**:e0180064.
39. Lal S, Li A, Allen D, Allen PD, Bannon P, Cartmill T, Cooke R, Farnsworth A, Keogh A, dos Remedios C. Best practice biobanking of human heart tissue. *Biophys Rev* 2015;**7**:399–406.
40. Marston S, Montgiraud C, Munster AB, Copeland O, Choi O, dos Remedios C, Messer AE, Ehler E, Knöll R. OBSCN mutations associated with dilated cardiomyopathy and haploinsufficiency. *PLoS One* 2015;**10**:e0138568.
41. Love MI, Huber W, Anders S. Moderated estimation of fold change and dispersion for RNA-seq data with DESeq2. *Genome Biol* 2014;**15**:550.
42. Prieto C, Barrios D. RaNA-Seq: interactive RNA-Seq analysis from FASTQ files to functional analysis. *Bioinformatics* 2019.
43. Anders S, Reyes A, Huber W. Detecting differential usage of exons from RNA-seq data. *Genome Res* 2012;**22**:2008–2017.
44. Kinoshita E, Kinoshita-Kikuta E, Takiyama K, Koike T. Phosphate-binding tag, a new tool to visualize phosphorylated proteins. *Mol Cell Proteomics* 2006;**5**:749–757.
45. Vikhorev PG, Ferenczi MA, Marston SB. Instrumentation to study myofibril mechanics from static to artificial simulations of cardiac cycle. *MethodsX* 2016;**3**:156–170.
46. de Tombe PP, Stienen GJ. Impact of temperature on cross-bridge cycling kinetics in rat myocardium. *J Physiol* 2007;**584**:591–600.
47. de Tombe PP, Stienen GJ. Protein kinase A does not alter economy of force maintenance in skinned rat cardiac trabeculae. *Circ Res* 1995;**76**:734–741.
48. Pappas CT, Mayfield RM, Henderson C, Jamilpour N, Cover C, Hernandez Z, Hutchinson KR, Chu M, Nam KH, Valdez JM, Wong PK, Granzier HL, Gregorio CC. Knockout of Lmod2 results in shorter thin filaments followed by dilated cardiomyopathy and juvenile lethality. *Proc Natl Acad Sci USA* 2015;**112**:13573–13578.
49. Prill K, Carlisle C, Stannard M, Windsor Reid PJ, Pilgrim DB. Myomesin is part of an integrity pathway that responds to sarcomere damage and disease. *PLoS One* 2019;**14**:e0224206.
50. Collier MP, Alderson TR, de Villiers CP, Nicholls D, Gastall HY, Allison TM, Degiacomi MT, Jiang H, Mlynec G, Furst DO, van der Ven PFM, Djinoovic-Carugo K, Baldwin AJ, Watkins H, Gehrmlich K, Benesch JLP. HspB1 phosphorylation regulates its intramolecular dynamics and mechanosensitive molecular chaperone interaction with filamin C. *Sci Adv* 2019;**5**:eaav8421.
51. Gautel M, Zuffardi O, Freiburg A, Labeit S. Phosphorylation switches specific for the cardiac isoform of myosin binding protein-C: a modulator of cardiac contraction? *EMBO J* 1995;**14**:1952–1960.
52. Mangmool S, Parichatikanond W, Kurose H. Therapeutic targets for treatment of heart failure: focus on GRKs and β -arrestins affecting β AR signaling. *Front Pharmacol* 2018;**9**:1336.
53. Husberg C, Agnetti G, Holewinski RJ, Christensen G, Van Eyk JE. Dephosphorylation of cardiac proteins in vitro—a matter of phosphatase specificity. *Proteomics* 2012;**12**:973–978.
54. Martín-Garrido A, Biesiadecki BJ, Salhi HE, Shaifta Y, dos Remedios CG, Ayaz-Guner S, Cai W, Ge Y, Avkiran M, Kentish JC. Monophosphorylation of cardiac troponin-I at Ser-23/24 is sufficient to regulate cardiac myofibrillar Ca^{2+} sensitivity and calpain-induced proteolysis. *J Biol Chem* 2018;**293**:8588–8599.
55. Bristow MR. Why does the myocardium fail? Insights from basic science. *Lancet* 1998;**352**:S18–14.
56. Vikhorev PG, Vikhoreva NN. Cardiomyopathies and related changes in contractility of human heart muscle. *IJMS* 2018;**19**:2234.

57. Messer AE, Gallon CE, McKenna WJ, dos Remedios CG, Marston SB. The use of phosphate-affinity SDS-PAGE to measure the cardiac troponin I phosphorylation site distribution in human heart muscle. *Prot Clin Appl* 2009;**3**:1371–1382.
58. Kooij V, Holewinski RJ, Murphy AM, Van Eyk JE. Characterization of the cardiac myosin binding protein-C phosphoproteome in healthy and failing human hearts. *J Mol Cell Cardiol* 2013;**60**:116–120.
59. Bollen IAE, Schuldt M, Harakalova M, Vink A, Asselbergs FW, Pinto JR, Kruger M, Kuster DWD, van der Velden J. Genotype-specific pathogenic effects in human dilated cardiomyopathy. *J Physiol* 2017;**595**:4677–4693.
60. Memo M, Leung MC, Ward DG, dos Remedios C, Morimoto S, Zhang L, Ravenscroft G, McNamara E, Nowak KJ, Marston SB, Messer AE. Familial dilated cardiomyopathy mutations uncouple troponin I phosphorylation from changes in myofibrillar Ca(2)(+) sensitivity. *Cardiovasc Res* 2013;**99**:65–73.
61. Hamdani N, Borbely A, Veenstra SP, Kooij V, Vrydag W, Zaremba R, Dos Remedios C, Niessen HW, Michel MC, Paulus WJ, Stienen GJ, van der Velden J. More severe cellular phenotype in human idiopathic dilated cardiomyopathy compared to ischemic heart disease. *J Muscle Res Cell Motil* 2010;**31**:289–301.
62. Kooij V, Saes M, Jaquet K, Zaremba R, Foster DB, Murphy AM, Dos Remedios C, van der Velden J, Stienen GJ. Effect of troponin I Ser23/24 phosphorylation on Ca2+ sensitivity in human myocardium depends on the phosphorylation background. *J Mol Cell Cardiol* 2010;**48**:954–963.
63. Bollen IAE, Ehler E, Fleischanderl K, Bouwman F, Kempers L, Ricke-Hoch M, Hilfiker-Kleiner D, Dos Remedios CG, Kruger M, Vink A, Asselbergs FW, van Spaendonck-Zwarts KY, Pinto YM, Kuster DWD, van der Velden J. Myofilament remodeling and function is more impaired in peripartum cardiomyopathy compared with dilated cardiomyopathy and ischemic heart disease. *Am J Pathol* 2017;**187**:2645–2658.
64. Beqqali A, Bollen IA, Rasmussen TB, van den Hoogenhof MM, van Deutekom HW, Schafer S, Haas J, Meder B, Sorensen KE, van Oort RJ, Mogensen J, Hubner N, Creemers EE, van der Velden J, Pinto YM. A mutation in the glutamate-rich region of RNA-binding motif protein 20 causes dilated cardiomyopathy through missplicing of titin and impaired Frank-Starling mechanism. *Cardiovasc Res* 2016;**112**:452–463.
65. Wijnter PJ, Murphy AM, Stienen GJ, van der Velden J. Troponin I phosphorylation in human myocardium in health and disease. *Neth Heart J* 2014;**22**:463–469.
66. Hamdani N, Herwig M, Linke W. Tampering with springs: phosphorylation of titin affecting the mechanical function of cardiomyocytes. *Biophys Rev* 2017;**9**:225–237.
67. Nagueh SF, Shah G, Wu Y, Torre-Amione G, King NM, Lahmers S, Witt CC, Becker K, Labeit S, Granzier HL. Altered titin expression, myocardial stiffness, and left ventricular function in patients with dilated cardiomyopathy. *Circulation* 2004;**110**:155–162.
68. Ait-Mou Y, Hsu K, Farman GP, Kumar M, Greaser ML, Irving TC, de Tombe PP. Titin strain contributes to the Frank-Starling law of the heart by structural rearrangements of both thin- and thick-filament proteins. *Proc Natl Acad Sci USA* 2016;**113**:2306–2311.
69. Harada N, Okuyama M, Yoshikatsu A, Yamamoto H, Ishiwata S, Hamada C, Hirose T, Shono M, Kuroda M, Tsutsumi R, Takeo J, Taketani Y, Nakaya Y, Sakaue H. Endoplasmic reticulum stress in mice increases hepatic expression of genes carrying a premature termination codon via a nutritional status-independent GRP78-dependent mechanism. *J Cell Biochem* 2017;**118**:3810–3824.
70. Selcen D. Myofibrillar myopathies. *Neuromuscular Disorders* 2011;**21**:161–171.
71. Selcen D, Ohno K, Engel AG. Myofibrillar myopathy: clinical, morphological and genetic studies in 63 patients. *Brain* 2004;**127**:439–451.
72. Kimura A. Molecular genetics and pathogenesis of cardiomyopathy. *J Hum Genet* 2016;**61**:41–50.
73. Frank D, Kuhn C, Katus HA, Frey N. The sarcomeric Z-disc: a nodal point in signaling and disease. *J Mol Med* 2006;**84**:446–468.
74. Bertz M, Wilmanns M, Rief M. The titin-telethonin complex is a directed, superstable molecular bond in the muscle Z-disk. *Proc Natl Acad Sci USA* 2009;**106**:13307–13310.
75. Lyon RC, Zanella F, Omens JH, Sheikh F. Mechanotransduction in cardiac hypertrophy and failure. *Circ Res* 2015;**116**:1462–1476.
76. Ujfalusi Z, Vera CD, Mijailovich SM, Svicevic M, Yu EC, Kawana M, Ruppel KM, Spudich JA, Geeves MA, Leinwand LA. Dilated cardiomyopathy myosin mutants have reduced force-generating capacity. *J Biol Chem* 2018;**293**:9017–9029.
77. Piroddi N, Witjas-Paalberends ER, Ferrara C, Ferrantini C, Vitale G, Scellini B, Wijnter PJM, Sequiera V, Dooijes D, dos Remedios C, Schlossarek S, Leung MC, Messer A, Ward DG, Biggeri A, Tesi C, Carrier L, Redwood CS, Marston SB, van der Velden J, Poggesi C. The homozygous K280N troponin T mutation alters cross-bridge kinetics and energetics in human HCM. *J Gen Physiol* 2019;**151**:18–29.
78. Ferrantini C, Coppini R, Pioner JM, Gentile F, Tosi B, Mazzoni L, Scellini B, Piroddi N, Laurino A, Santini L, Spinelli V, Sacconi L, de Tombe P, Moore R, Tardiff J, Mugelli A, Olivetto I, Cerbai E, Tesi C, Poggesi C. Pathogenesis of hypertrophic cardiomyopathy is mutation rather than disease specific: a comparison of the cardiac troponin T E163R and R92Q mouse models. *JAMA* 2017;**6**:e005407.
79. Narolska NA, van Loon RB, Boontje NM, Zaremba R, Penas SE, Russell J, Spiegelberg SR, Huybregts MA, Visser FC, de Jong JW, van der Velden J, Stienen GJ. Myocardial contraction is 5-fold more economical in ventricular than in atrial human tissue. *Cardiovasc Res* 2005;**65**:221–229.
80. Bombardini T, Gemignani V, Bianchini E, Venneri L, Petersen C, Pasanisi E, Pratali L, Alonso-Rodriguez D, Pianelli M, Fata F, Giannoni M, Arpesella G, Picano E. Diastolic time—frequency relation in the stress echo lab: filling timing and flow at different heart rates. *Cardiovasc Ultrasound* 2008;**6**:15.
81. Beer M, Seyfarth T, Sandstede J, Landschutz W, Lipke C, Kostler H, von Kienlin M, Harre K, Hahn D, Neubauer S. Absolute concentrations of high-energy phosphate metabolites in normal, hypertrophied, and failing human myocardium measured non-invasively with (31)P-SLOOP magnetic resonance spectroscopy. *J Am Coll Cardiol* 2002;**40**:1267–1274.

Translational perspective

Our findings may have implications in the development of new strategies for DCM treatment in patients with *TTN*-truncating variants as well as in the development of new drugs.